International Journal of Mass Spectrometry 316–318 (2012) 259–267

Contents lists available at SciVerse ScienceDirect

International Journal of Mass Spectrometry

journal homepage: www.elsevier.com/locate/ijms

Influence of a gamma amino acid on the structures and reactivity of peptide a_3 ions

Matthew C. Bernier[a], Bela Paizs[a,b,*], Vicki H. Wysocki[a,**]

[a] Department of Chemistry and Biochemistry, University of Arizona, Tucson, AZ 85721, United States
[b] Computational Proteomics Group, German Cancer Research Center, Im Neuenheimer Feld 580, 69120 Heidelberg, Germany

ARTICLE INFO

Article history:
Received 10 December 2011
Received in revised form 25 February 2012
Accepted 28 February 2012
Available online 7 March 2012

Keywords:
Peptides
Collision induced dissociation
Fragmentation
Density functional theory
Relative energies

ABSTRACT

Collision-induced dissociation of protonated AGabaAIG (where Gaba is gamma-amino butyric acid, NH_2–$(CH_2)_3$–COOH) leads to an unusually stable a_3 ion. Tandem mass spectrometry and theory are used here to probe the enhanced stability of this fragment, whose counterpart is not usually observed in CID of protonated peptides containing only alpha amino acids. Experiments are carried out on the unlabelled and ^{15}N-Ala labeled AGabaAIG (labeled separately at residue one or three) probing the b_3, a_3, a_3-NH_3 (a_3^*), and b_2 fragments while theory is used to characterize the most stable b_3, a_3, and b_2 structures and the formation and dissociation of the a_3 ion. Our results indicate the AGabaA oxazolone b_3 isomer undergoes head-to-tail macrocyclization and subsequent ring opening to form the GabaAA sequence isomer while this chemistry is energetically disfavored for the AAA sequence. The AGabaA a_3 fragment also undergoes macrocyclization and rearrangement to form the rearranged imine–amide isomer while this reaction is energetically disfavored for the AAA sequence. The barriers to dissociation of the AGabaA a_3 ion via the $a_3 \rightarrow b_2$ and $a_3 \rightarrow a_3^*$ channels are higher than the literature values reported for the AAA sequence. These two effects provide a clear explanation for the enhanced stability of the AGabaA a_3 ion.

1. Introduction

A great deal of research has focused on understanding how gas-phase peptide ions fragment upon activation in collision induced dissociation (CID). Studies on the structures and reactivities of peptide fragments are of great importance due to the widespread use of tandem mass spectrometry (MS/MS) for the identification of proteins in proteomics. In proteomic analyses, proteins are first broken down into peptides by enzymatic digestion generating a mixture of peptides. This mixture is then separated by HPLC and subsequently analyzed by automated MS/MS. Peptide ions are typically subjected to CID, where energy is imparted into the ion by collisions with a neutral gas and the ion then fragments producing product ion spectra [1,2]. CID predominantly forms fragments by breaking the peptide bonds leading to *b* and *y* ions [3,4], with the former often fragmenting further to *a* ion fragments. The information encoded in the observed mass-to-charge ratios is then used to decipher sequences, mostly by automated bioinformatics tools. Most software assumes an even distribution of cleavage probabilities for the amide bonds and will compare such theoretical spectra, or even simple *m*/*z* lists with little or no intensity information, to experimental fragmentation patterns to identify the peptide sequence. Recent research efforts by the gas-phase ion chemistry community are aimed at greater understanding of why certain peptide fragments are formed and elucidation of the mechanisms that guide this fragmentation [5]. It has been proposed that this information can be used to improve the current sequencing/identification software and therefore could lead to improved data-processing in large-scale proteomics projects.

While recent studies have shed light on fine details of the formation, structures, and reactivities of *b* fragments [6–11], relatively less is known about *a* fragments [12–25]. It is generally accepted that a_n ions typically result by CO loss from the oxazolone isomer of b_n fragment ions [12,16,17] as proposed by Harrison. The resulting imine isomer (—CO—HN^+=CH—R_n) has a linear backbone; e.g. CO is eliminated from the C-terminal oxazolone ring of the b_n ions in the $b_n \rightarrow a_n$ reaction [15,18]. The imine isomer a_n ions are reactive and can undergo a variety of rearrangement and fragmentation reactions. In order to determine their most stable structures recent studies employed infrared multi-photon dissociation (IRMPD) spectroscopy [8,23–25] and ion mobility spectrometry [20] both combined with extensive modeling. These investigations indicated that the linear imine isomer of a_n ions can undergo head-to-tail cyclization [8] forming a macrocyclic isomer with a backbone composed of a secondary amine and amide

* Corresponding author at: Computational Proteomics Group, German Cancer Research Center, Im Neuenheimer Feld 580, 69120 Heidelberg, Germany.
** Corresponding author.
E-mail addresses: B.Paizs@dkfz.de (B. Paizs), vwysocki@email.arizona.edu (V.H. Wysocki).

1387-3806/$ – see front matter © 2012 Elsevier B.V. All rights reserved.
doi:10.1016/j.ijms.2012.02.028

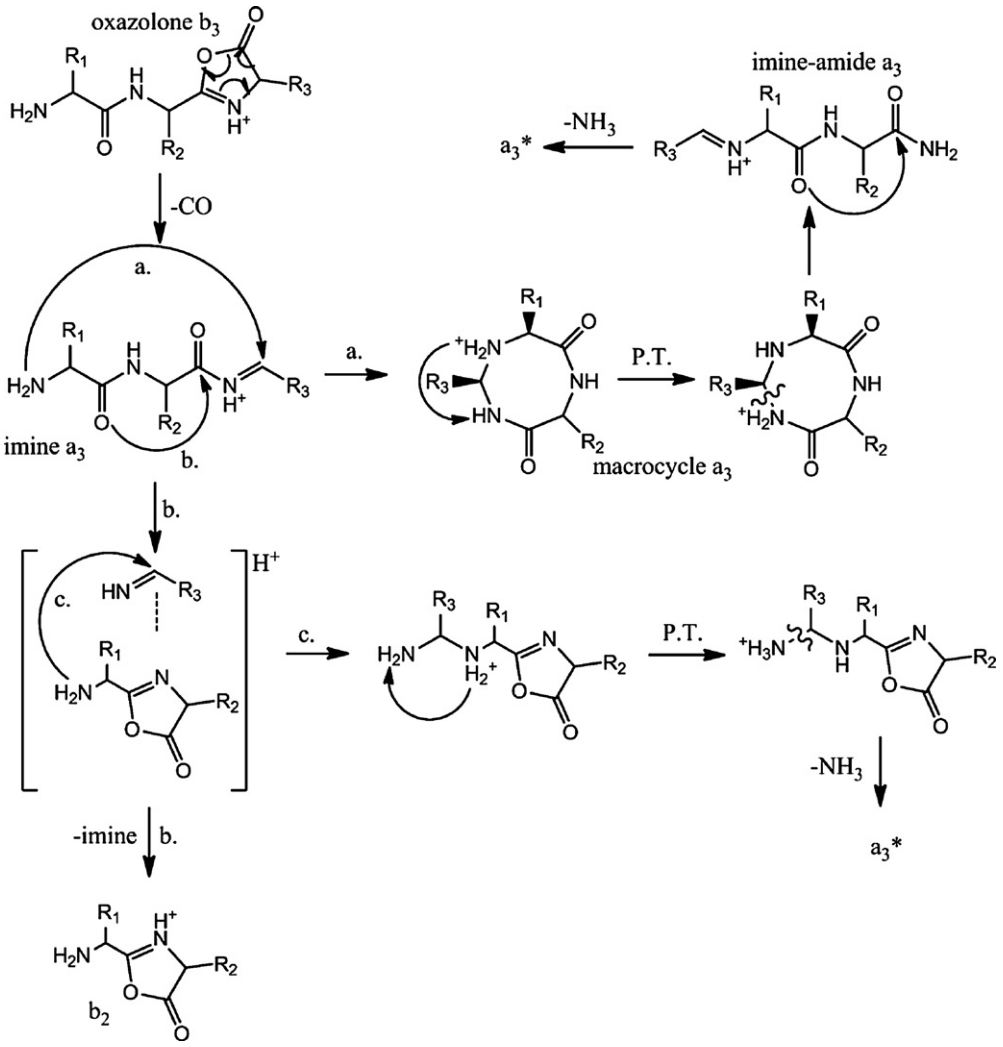

Scheme 1. Possible fragmentation pathways for formation of a_3 and its subsequent fragments proposed in the literature [14,18,22,24].

groups. This macrocyclic isomer can open up to reform the original linear imine or, after proton transfer to the amide nitrogen adjacent to the secondary amine, to a rearranged 'imine–amide' isomer [23]. These a_3 pathways as well as the formation of a_3 from b_3 are shown in Scheme 1. Theoretical studies indicate the macrocyclic isomer as energetically favored or more favored than the linear imine and the rearranged 'imine–amide' structure is much more favored than the first two. The actual abundance ratios of these structures depend on the experimental conditions under which the a_n ions are formed and probed [25]. For example, ion mobility data [20] on the a_4 of protonated YGGFL indicate the presence of all three structures while a recent IR spectroscopy study performed in an ion trap on the same ion indicates dominance of the 'imine–amide' isomer [25].

Two major dissociation reactions of a_n ions are described in the literature including elimination of ammonia to form the a_n-NH_3 (a_n^*) [15] ion and fragmentation to the next-lower *b* ion, the b_{n-1} ion [19]. A mechanism proposed previously, which is shown on pathway b of Scheme 1, suggests the b_{n-1} can be formed via attack of the closest N-terminal carbonyl oxygen on the carbonyl carbon N-terminal to the protonated imine [19] leading to loss of the C-terminal imine and formation of Harrison's stable linear oxazolone b_{n-1}. There is greater debate about what mechanism leads to a_n^* formation. It was previously proposed by Glish and coworkers [15] that this ion was formed after proton transfer to the N-terminus of the linear form by elimination of the N-terminal $-NH_3^+$ as ammonia upon attack of the C-terminal imine nitrogen by an S_N2 reaction that forms a macrocycle, which has a fixed charge at the original imine nitrogen that could in principle unfold to an acylium (or rather oxazolone terminated) a_n^* ion [15], as shown in Scheme 1 pathway a. More recently, Cooper et al. [18] proposed an alternative mechanism, described in Scheme 1 by pathway c, that leads to elimination of the imine nitrogen (e.g. not the N-terminal amine nitrogen) in the departing ammonia. The process is initiated via nucleophilic attack by the N-terminal adjacent carbonyl oxygen on the carbonyl carbon adjacent to the C-terminal imine, e.g. via the same reaction that leads to the b_{n-1} ion. Before complete loss of the imine to form b_{n-1}, however, a proton-bound dimer (PBD) of the two fragments is formed. This PBD can rearrange bringing the imine close to the N-terminus of the b_{n-1} fragment where it covalently binds via a C—N bond. This new re-associated structure can then undergo a proton transfer to give an NH_3 group that is easily lost [18]. Site-specific ^{15}N labeling of the FGGFL peptide was used to probe the S_N2 and PBD ammonia elimination reactions; only the latter was compatible with the labeling data indicating that the former pathway is not active [22]. Another mechanism for the ammonia elimination was proposed recently [26] from the rearranged 'imine–amide' a_n structures (see above). Formally, these have the R_n—CH=NH^+—CHR_1—···—CO—NH_2 backbone and if the ionizing proton is transferred to the C-terminal amide nitrogen R_n—CH=N—CHR_1—···—CO—NH_3^+ is formed from which NH_3 is eliminated by attack of the N-terminal adjacent carbonyl oxygen.

One unusual trend in the chemistry of a_n ions is the low intensity of the a_3 fragment ions compared to that of other a_n fragments. Glish and co-workers [21] analyzed 29 peptides and discovered that the CID spectra of the majority of these did not feature the a_3 fragment while a_2 and a_4 were present under the same CID conditions. Using a theoretical approach, Glish and coworkers investigated the $b_4 \rightarrow a_4 \rightarrow b_3 \rightarrow a_3 \rightarrow b_2 \rightarrow a_2 \rightarrow a_1$ reaction cascade and concluded that the barrier to the $a_3 \rightarrow b_2$ reaction was significantly lower than to those of $a_4 \rightarrow b_3$ and $a_2 \rightarrow a_1$, making the a_3 structure easily convertible to the more stable b_2. Concurrently, Zubarev and co-workers [27] reached the same conclusion in a statistical analysis of a large spectral database collected in studies on human and *Escherichia coli* cell lysates. Two trends were observed in these data: one that showed the high frequency of the b_2 ions in the b_n series and one that showed significantly reduced frequency of a_3 compared to the rest of the a_n ion series. Zubarev and coworkers explained the latter by formation of alternative (cyclic peptide isomer) b_2 ions and their increased stability compared to other b_n fragments. Moreover, an IR spectroscopy study performed in an ion trap did observe a stable a_3 ion from the GGGG peptide [25]. It was established to be a seven-membered cyclic isomer formed from the linear imine structure by attack of the N-terminal amide oxygen on the carbon center of the N-terminal imine. It is worth noting here that the metastable ion spectra of the b_3 ions of protonated AAAAA and YGGFL feature abundant a_3 fragments that are likely very fragile because their abundance becomes very low even under mild CID conditions [13].

Previous studies of this 'a_3 phenomenon' have focused on peptides composed exclusively of alpha amino acids. Here we present experimental and theoretical data on peptides containing gamma-amino butyric acid (Gaba, NH_2—$(CH_2)_3$—COOH), AGabaAIG and GabaAAIG. The Gaba amino acid increases the length of the backbone by two methylenes, and was chosen to create an artificially less kinetically favored seven-membered ring b_2 ion instead of the five-membered oxazolone ring of the b_2 ion, potentially encouraging retention of the a_3 fragment. In fact, in the product ion spectra of protonated AGabaAIG the a_3 ion is present as one of the most abundant fragments, while the GabaAAIG does not form abundant a_3 ions upon CID. The peptides were terminated with -IG since it was believed, based on statistical analysis in our group, that this ending sequence could provide a high b_3 ion intensity with the potential to provide high a_3 ion intensity. By studying the formation, structure and reactivity of the related AGabaA and GabaAA a_3 ions we aim to better understand the chemistry of a_3 ions in general.

2. Experimental

All peptides were synthesized using standard Fmoc solid-phase synthesis [28] with all unlabeled, protected amino acids purchased from EMD Biosciences or ChemPep. Fmoc-^{15}N-Ala-OH was purchased from Sigma–Aldrich and used in the same solid phase synthesis method to produce (^{15}N-A)GabaAIG and AGaba(^{15}N-A)IG. All peptides were synthesized and then diluted in 50:50 H_2O:ACN solution with 0.1% formic acid to concentrations of approximately 10–50 μM.

The mass spectra were collected on a modified Waters Synapt G2 in positive ion mode using electrospray ionization. The source voltage was set between 3 and 4 kV with cone and extractor voltages set to ~30 V and ~5 V, respectively. Ions were selected in the initial quadrupole and fragmentation performed with argon gas in the trap stacked ring ion guide located immediately before the IMS cell of the instrument. Although not used in this study, the instrument has been modified with a surface-induced dissociation (SID) device [29] placed between the IMS cell and a shortened transfer cell. To perform pseudo MS^3 fragmentation, the sampling cone voltage was raised 20–30 V and resulting fragments isolated by the quadrupole with trap CID occurring afterwards.

Additional experiments were performed in a Bruker APEX Qe 9.4 T FTICR. MS^3 was achieved through fragmentation of the peptide ions in source, isolation of the investigated fragment in the ICR and inducing further fragmentation by SORI-CID. All precursor peptides were ionized via electrospray ionization at 4.8 kV. SORI-CID was performed in the ICR cell after source fragmentation, where power percentages stayed at 1.2–1.5% of their maximum excitation with the length of each SORI pulse set at 0.3 s. Quadrupole isolation was unnecessary for precursor or fragments, since there was sufficient source energy to result in each CID ion, which was then isolated in the cell.

3. Computational details

Maestro (version 9.1) was used to build the starting structures for all fragments [30]. In order to generate a number of starting structures for further quantum chemical calculations, a conformation search was done with a Monte Carlo mixture model (MCMM) using the Merck molecular force field MMFF with the torsional sampling option from the Schrodinger software program Macromodel [31]. The MCMM conformational method is an algorithm that explores geometries generated by randomly changing torsion angles which are then energy optimized and either considered a valid structure or not based on a number of parameters [32]. This process is repeated a specified number of times based on user preference. In our conformational search, 10,000 structures were generated with 2500 steps per rotatable bond. Of the 10,000 structures generated, a cut-off of 1.0–2.0 Å atom deviation was set up and redundant structures were removed. Between 10 and 20 starting structures, selected based on representative hydrogen bonding and torsional features, were chosen from the 100–200 minimized structures to be run at the PM3 and higher optimizations. To calculate energies of each structure at the PM3, HF/3-21G, B3LYP/6-31G(d), and B3LYP/6-31+G(d,p) theoretical levels, the Gaussian 09 program was used [33]. Stepwise calculations going from lower theoretical levels to higher allowed for faster calculation speeds at each theoretical level and the removal of redundant structures. The final reported energy values were determined at the B3LYP/6-31+G(d,p) level, zero-point energy and other thermochemical corrections were obtained from vibrational frequencies calculated at the B3LYP/6-31G(d) level. Relative Gibbs free energies were calculated at 298 K.

4. Results and discussion

4.1. CID of protonated AGabaAIG, GabaAAIG, and AAAIG

The CID spectra of protonated AGabaAIG, GabaAAIG, and AAAIG are shown in Fig. 1. Both Gaba precursor ions (m/z at 416.25) give a variety of b_n and a_n fragments indicating facile dissociation at the backbone amide bonds. The product ion spectrum of protonated GabaAAIG (Fig. 1b) is dominated by the b_2 ion at 22 eV collision energy (laboratory frame) with the b_4, a_4, b_3, and $a_3{}^*$ fragments being less abundant. The CID behavior of this peptide is 'usual' in terms of the 'a_3 phenomenon' because no significant peak is observed at the expected m/z (200) of the a_3 ion. The fragmentation pattern of protonated AGabaAIG (Fig. 1a) significantly differs from that of protonated GabaAAIG. The base peak at 22 eV collision energy is the a_3 ion. Therefore, CID of protonated AGabaAIG is 'unusual' in terms of the 'a_3 phenomenon'. Furthermore, the $a_3{}^*$ ion is more abundant than it is in CID of protonated GabaAAIG and fragments at m/z 140.1, 139.1, and 112.1, which were not present in the GabaAAIG case, are present. The MSMS spectrum of AAAIG,

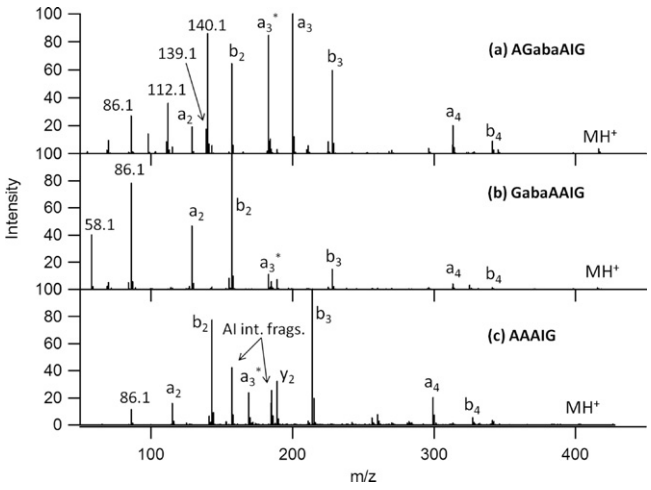

Fig. 1. Product ion mass spectra of protonated (a) AGabaAIG, (b) GabaAAIG, and (c) AAAIG recorded on the G2 Synapt instrument at 22 eV collision energy (laboratory frame).

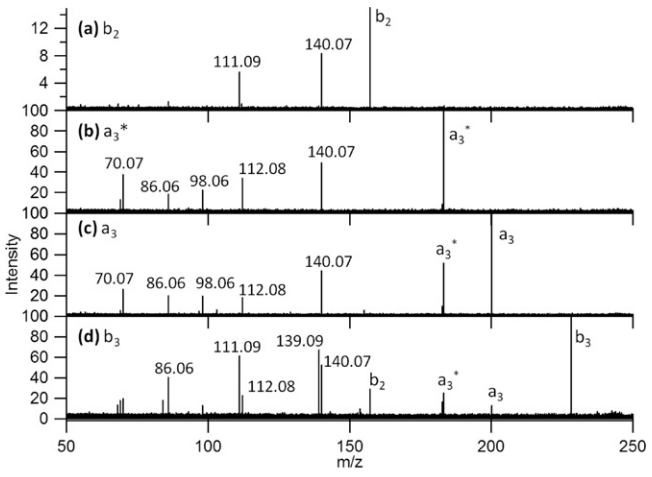

Fig. 2. MS^3 tandem mass spectra (recorded using SORI-CID after source fragmentation) of (a) the b_2, (b) the $a_3{}^*$, (c) the a_3 and (d) the b_3 fragment ions of protonated AGabaAIG.

shown in Fig. 1c, is added to explain that the behavior of the standard Ala containing version of the model peptide does in fact show no significant a_3 ion intensity. At the same conditions of 22 eV collision energy in the G2 Synapt, this 'normal' peptide has significant ion intensity at the b_3 followed in abundance by the b_2.

Fig. S1 in the Supporting Information shows energy resolved mass spectra (ERMS) graphs for both Gaba peptides. These are again different, with that of protonated GabaAAIG similar to ERMS graphs observed for similar peptides with alpha amino acids [13,19] and with that of protonated AGabaAIG rather different from those literature cases. Again, the ERMS of the AAAIG (not shown) shows no significant a_3 intensity throughout the range of collision energies. The most striking difference between the two graphs in Fig. S1, besides the lack of a_3 in the GabaAAIG case and dominance of the a_3 species in the AGabaAIG case, is the prevalence of the b_2 ion in the former. This suggests that the b_2 ion with the GabaA sequence is kinetically favored or very stable or both. It is also worth noting that $a_3{}^*$ is much less abundant in the GabaAAIG case than in AGabaAIG for the whole collision energy range studied. These observations indicate that the fragmentation chemistries of protonated AGabaAIG and GabaAAIG are rather different. Substitution of an alanine residue by Gaba in the AAA sequence and therefore expansion of the backbone by two methylene groups produces a rarely seen a_3 fragment when on the second position but gives instead a very stable b_2 when on the first position. In order to further understand the effects this backbone extension can have on fragment ion formation, MS^3 studies were performed on selected fragments of protonated AGabaAIG.

4.2. CID of the b_3, a_3, $a_3{}^*$, and b_2 fragments of protonated AGabaAIG

Fig. 2 displays the results of CID experiments performed on b_3, a_3, $a_3{}^*$, and b_2 of protonated AGabaAIG. Both the b_3 and a_3 spectra show abundant formation of $a_3{}^*$ and the fragment at m/z 140.07. CID of a_3 features only a marginally abundant b_2 peak at m/z 157.10 while CID of b_3 has a moderately abundant peak at this position. CID of $a_3{}^*$ results in two major peaks, at m/z 140.07 and 112.08, respectively, indicating that these ions appear to be part of the $a_3 \rightarrow a_3{}^* \rightarrow m/z$ 140.07 cascade. However, a m/z 140.07 fragment also is observed in CID of b_2 and it is not clear without additional data whether this is a structurally different isomer or has the same structure as m/z 140.07 in CID of $a_3{}^*$. Additionally, the b_3 MS^3 spectrum in Fig. 2d shows a peak at m/z 139.09 not present in the a_3, $a_3{}^*$ or b_2 spectra and a peak at m/z 111.09 that is observed only in CID of b_2. This indicates the m/z 139.09 is formed on a pathway specific to the b_3 ion or that the energetics for each starting fragment ion can drastically affect the intensity of the ions within a particular cascade. The latter is a likely possibility since the MS^3 of the m/z 139.09 fragment contains the m/z 111.09 ion as well (spectrum not shown).

4.3. CID of fragments of protonated (^{15}N-A)GabaAIG, AGaba(^{15}N-A)AIG, and N-terminally acetylated AGabaAIG

CID of isotopically labeled peptides has been successfully applied to probe the dissociation pathways of a few b_n and a_n ions [18,22]. For example, the formation of $a_3{}^*$ of protonated GGGG was probed by studying CID after labeling the N-terminal Gly with ^{15}N. These experiments demonstrated that it is not the N-terminal amino nitrogen, but rather the nitrogen of the third Gly that is eliminated as NH_3 in the $a_3 \rightarrow a_3{}^*$ reaction. CID of protonated GGGG is 'usual' in terms of the 'a_3 phenomenon' because the a_3 signal is observed only under very mild CID conditions [23]. In order to further probe the chemistry behind the 'unusual' 'a_3 phenomenon' featured in CID of protonated AGabaAIG, the N-terminus of AGabaAIG was acetylated and AGaba(^{15}N-A)IG and (^{15}N-A)GabaAIG were synthesized and their dissociation pathways were investigated by CID. The main goal of these experiments was to determine which nitrogen was lost as ammonia in CID of the AGabaAIG peptide and whether the nitrogen could be lost if the N-terminus was blocked. Figs. 3–5 show the CID spectra of the b_3, a_3 and b_2 ions of the two isotopically labeled peptides while Fig. S2 (Supporting Information) shows the product ion spectrum of the acetylated unlabeled peptide.

As expected, the m/z values of the a_3 and b_3 ions are the same for the (^{15}N-A)GabaAIG and AGaba(^{15}N-A)IG cases (Fig. 3) because these are both labeled with ^{15}N. The fragments located at lower m/z, however, show significant differences between the two spectra. For example, $a_3{}^*$ appears dominantly at m/z 184.1 for (^{15}N-A)GabaAIG and as a doublet of m/z 183.1 and 184.1 dominated by the former when generated from b_3 of AGaba(^{15}N-A)IG. Similarly, we observe a splitting of the formal b_2 peak in both cases. Most interestingly, the peak pairs 111.09 and 112.08 and 139.09 and 140.07 observed for the unlabeled AGabaAIG and for (^{15}N-A)GabaAIG merge in the AGaba(^{15}N-A)IG case under unit resolution but appear as separate peaks if high resolution spectra are acquired (see inset in Fig. 3b).

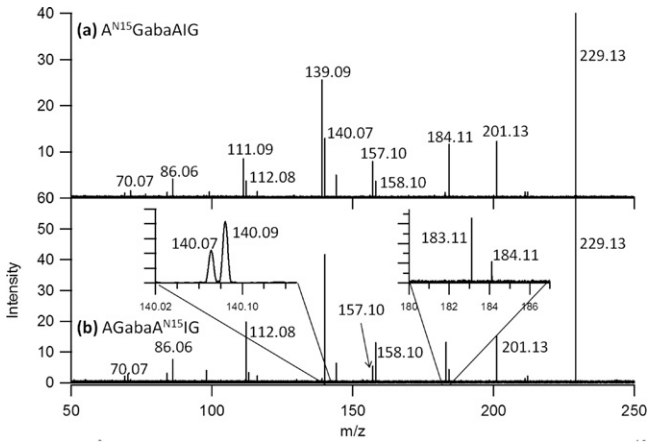

Fig. 3. MS^3 tandem mass spectra (recorded using SORI-CID) of (a) the b_3 of protonated (^{15}N-A)GabaAIG and (b) the b_3 of protonated AGaba(^{15}N-A)IG. Insets in (b) are expanded ranges of the m/z 140 and m/z 180–187 regions.

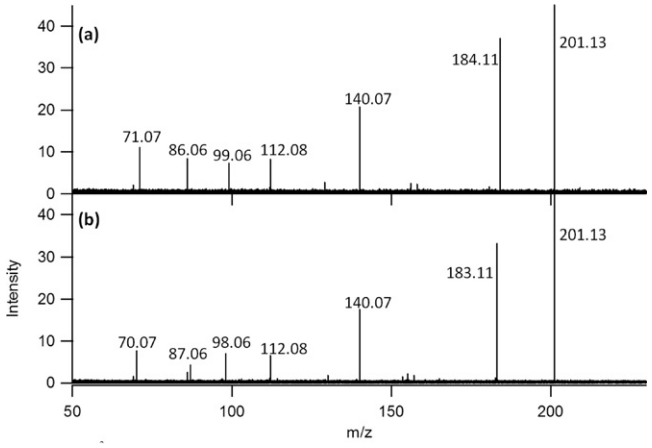

Fig. 4. MS^3 tandem mass spectra (recorded using SORI-CID) of m/z 201.13 (a) the a_3 of protonated (^{15}N-A)GabaAIG and (b) the a_3 of protonated AGaba(^{15}N-A)IG.

Isolation and CID of the a_3 ions of protonated (^{15}N-A)GabaAIG and AGaba(^{15}N-A)IG (Fig. 4) provide unambiguous information on the ammonia elimination reaction; $^{14}NH_3$ is eliminated from the former and $^{15}NH_3$ is eliminated from the latter. This clearly indicates that the nitrogen of the third Ala residue is eliminated as ammonia from stable (e.g. isolable) a_3 ions. The formal b_2 fragment

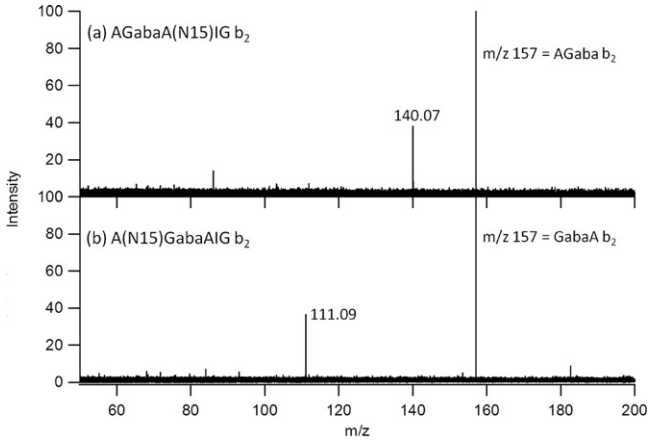

Fig. 5. MS^3 tandem mass spectra (recorded using SORI-CID) of the m/z 157.1 fragment of (a) protonated (^{15}N-A)GabaAIG and (b) protonated AGaba(^{15}N-A)IG.

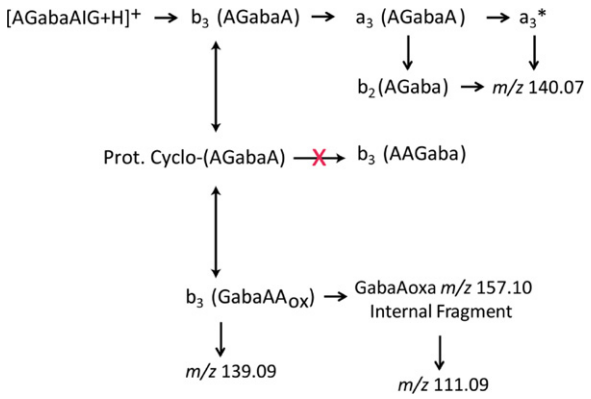

Scheme 2. Fragmentation pathways of protonated AGabaA b_3 ion.

of AGabaAIG appears as a doublet in CID of the b_3 ions of protonated (^{15}N-A)GabaAIG and AGaba(^{15}N-A)IG (Fig. 3). Fig. 5 shows CID of the m/z 157.10 component of this doublet for (^{15}N-A)GabaAIG and AGaba(^{15}N-A)IG. In the former case one observes only loss of ammonia while in the latter only formation of m/z 111.09. This indicates these two m/z 157.10 ions have different structures and the m/z 157.10 ion of protonated unlabeled AGabaAIG is composed of two structural isomers.

Comparing the CID spectrum of AGabaAIG (Fig. 1a) to its N-terminally acetylated form (Fig. S2) also shows distinct differences. The CID of protonated acetyl-AGabaAIG (m/z 458.28) recorded at 20 eV collision energy (laboratory frame) has a base peak at the b_1 fragment, which is only possible due to the acetyl group on the N-terminus. The next most intense peak is the a_3 ion and the spectrum also features b_2, b_3, a_4, b_4, m/z 86.1, m/z 129.1, and m/z 157.1 peaks. Of particular interest in this spectrum is that there is no significant a_3^* ion intensity observed. With the addition of an acetyl group blocking the N-terminus, the 'a_3 phenomenon' is still entirely possible, but the ammonia loss from the a_3 fragment ion becomes very unfavorable.

4.4. Formation, structure, and fragmentation pathways of the a_3 of protonated AGabaAIG

The product ion spectra of protonated AGabaAIG and acetyl-AGabaAIG and the b_3, a_3, a_3^* and b_2 ions of protonated AGabaAIG, (^{15}N-A)GabaAIG, and AGaba(^{15}N-A) provide detailed information on the related dissociation and rearrangement reactions that are summarized in Scheme 2. In the following, we will discuss the corresponding structures and reactions with the help of theoretical data obtained in modeling and quantum chemical calculations.

Dissociation of protonated AGabaAIG at the A—I amide bond leads to the oxazolone isomer b_3 ion with the AGabaA sequence ($AGabaA_{ox}$) that is expected to fragment further to form the unusually stable a_3 fragment. The b_3 ion either undergoes dissociation to form a_3 on the $b_3 \rightarrow a_3$ pathway or head-to-tail cyclization [34] to form the corresponding protonated cyclo-(AGabaA) isomer. The latter reaction is energetically not favored for the b_3 ion with the AAA sequence [21], however the increased flexibility of the AGabaA b_3 due to the two extra backbone methylenes allows formation of the eleven-membered macro-ring. Our calculations indicate the macrocyclic b_3 ion isomer (structure B in Chart 1) is only slightly less favored (2.4 kcal/mol) than the energetically most favored linear form (structure A, C-terminal oxazolone protonation). This is in clear contrast to the AAA case [21] where the linear vs. macrocyclic energy gap is more than 20.0 kcal/mol. The isomeric seven-membered ring terminated AAGaba form (structure D in Chart 1) is energetically much less favored than the oxazolone terminated AGabaA species; this

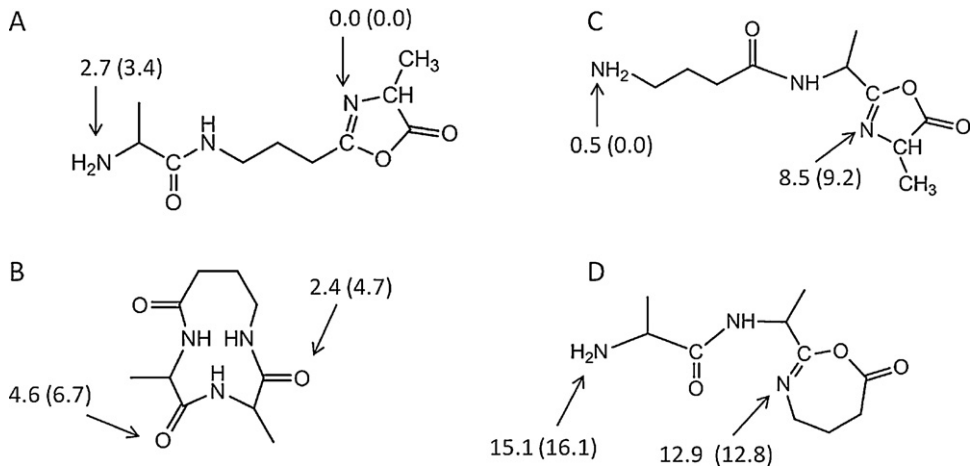

Chart 1. Various structures for the b_3 fragment of protonated AGabaAIG: (A) linear AGabaA isomer terminated by the oxazolone ring; (B) protonated cyclo-(AGabaA); (C) linear GabaAA isomer terminated by the oxazolone ring; (D) linear AAGaba isomer terminated by a seven-membered ring. Characterized protonation sites are indicated by arrows with the corresponding relative energies (kcal/mol) and relative Gibbs free energies (in parentheses, kcal/mol). The relative energies are calculated with respect to the oxazolone protonated AGabaA$_{ox}$ species A.

demonstrates the superior stability of Harrison's oxazolone ring [12,13] over seven-membered ring structures. Formation of a seven-membered ring is also kinetically less favorable than formation of a five-membered ring; because CID is a kinetic process, this must also be considered. On the other hand, the amino protonated GabaAA form (structure C in Chart 1) is energetically nearly as favored as AGabaA$_{ox}$. These theoretical data indicate that while AAGaba is particularly less favored as a seven-membered ring terminated structure, one should consider both the AGabaA$_{ox}$ and GabaAA$_{ox}$ sequence isomers when considering dissociation products of b_3.

Experimental evidence for the head-to-tail cyclization and ring-opening to form the GabaAA$_{ox}$ b_3 ion is delivered by CID of the b_3 and b_2 ions of the isotopically labeled peptides. In Fig. 3, one observes splitting of the formal b_2 peak into m/z 157.1 and 158.1 in both panels. The fate of the labeled Ala nitrogen is explicitly followed in Schemes S1 and S2; briefly CID of b_3 with the (^{15}N-A)GabaA sequence gives (^{15}N-A)Gaba b_2 (m/z 158.1) and after scrambling the GabaA$_{ox}$ internal ion (m/z 157.1). The peak at m/z 157.1 is more abundant than the peak at m/z 158.1, e.g. the internal ion GabaA$_{ox}$ is formed preferentially. Similar conclusions can be drawn from analysis of Fig. 3b based on Scheme S2. Furthermore, CID data presented in Fig. 5 for the m/z 157 ions from protonated (^{15}N-A)GabaAIG and AGaba(^{15}N-A)IG clearly indicate two isomeric structures. Exclusive loss of ammonia is in line with the AGaba isomer while formation of m/z 111.09 can be explained considering the GabaA sequence. Most likely this loss of m/z 46 is a combination of a water and carbonyl group, as makes sense given the exact mass work performed on the ICR. Furthermore, the DFT calculations performed on the relative energies of each possible b_2 ion structure shown in Chart 2 provide an explanation for the preferential formation of GabaA$_{ox}$ over other GabaA b_2 isomers. That is, GabaA$_{ox}$ is about 9 kcal/mol lower in energy than the AGaba b_2 isomer and 8 kcal/mol lower than the protonated AGaba head-to-tail cyclized structure. This energetic preference for the GabaA$_{ox}$ b_2 ion explains the dominance of this fragment in the CID of protonated GabaAAIG (Fig. 1a and S1) where this ion can directly be formed from the parent peptide and higher b ions without structural rearrangements.

Our theoretical work on the a_3 ion of protonated AGabaAIG focused on the AGabaA sequence formed from the AGabaA$_{ox}$ b_3 isomer. No detailed calculations were performed for the a_3 isomer with the GabaAA sequence because the GabaAAIG was shown to feature 'usual' behavior in terms of the 'a_3 phenomenon', e.g. negligible abundance. CID of protonated GabaAAIG does not lead to a prominent a_3 ion, and the b_2 is much more abundant then the a_3* indicating that the GabaAA a_3 ion dissociates preferentially to form the b_2. Therefore, there was no expected deviation from the ion structures and mechanisms previously discussed for a_3 ion chemistry [18,21,27]. The a_3 ion with the AGabaA sequence can be formed from the AGabaA$_{ox}$ b_3 isomer via the $b_3 \rightarrow a_3$ CO loss TS at 35.2 kcal/mol (Table S2) which is relatively comparable in energy to the reported AAA value of 31.7 kcal/mol for the same transition [21]. This indicates b_3 can easily convert to a_3 upon excitation and the Gaba residue at position two does not hinder this reaction channel.

In our calculations we considered most of the structures (Chart 3) proposed by Bythell et al. [23] for the a_3 ion of protonated GGGG. IR studies on that ion indicate it forms a cyclic structure generated by nucleophilic attack of the N-terminal amide oxygen on the carbon of the C-terminal imine. The corresponding AGabaA

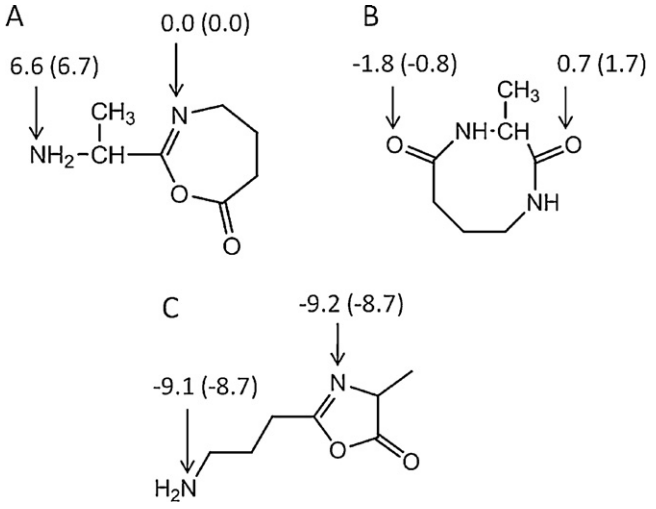

Chart 2. Structures for the b_2 fragment of protonated AGabaAIG and GabaAAIG: (A) linear AGaba isomer terminated by the seven-membered ring; (B) protonated eight-membered cyclo-(AGaba); (C) linear GabaA isomer terminated by the oxazolone ring. As with previous charts, protonation sites are indicated by arrows with the corresponding relative energies (kcal/mol) and relative Gibbs free energies (in parentheses, kcal/mol). The relative energies are calculated with respect to the ring nitrogen protonated AGaba species.

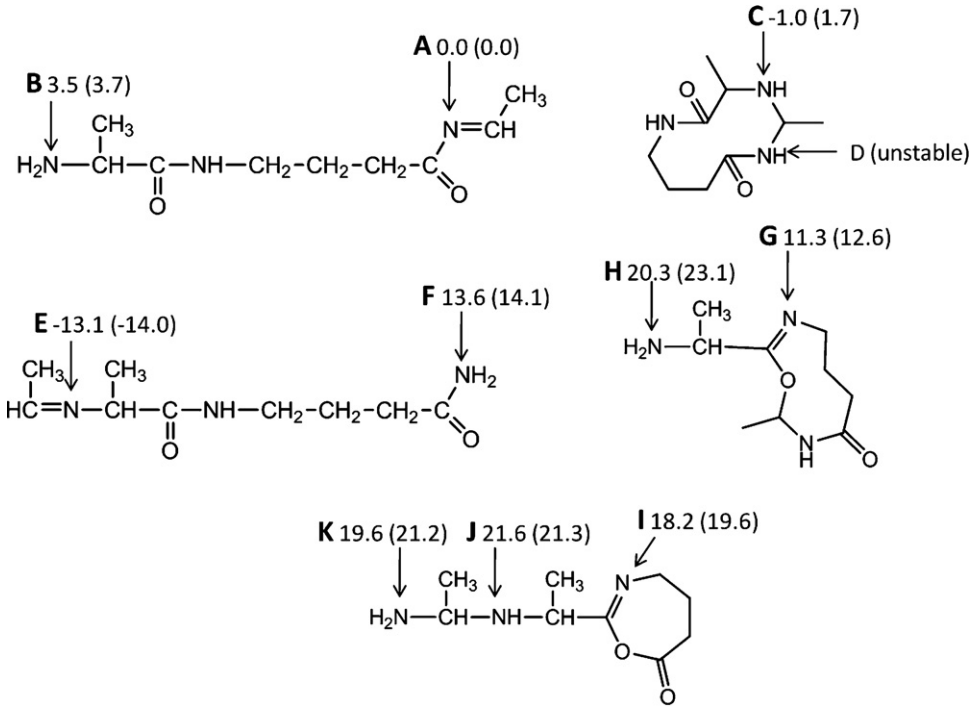

Chart 3. Various a_3 (AGabaA sequence) ion structures: (A, B) linear form protonated at the imine or N-terminal amino groups, respectively; (C, D) macrocyclic (eleven-membered ring) isomer protonated at the secondary amine or the adjacent amide nitrogen, respectively; (E, F) rearranged linear form protonated at the N-terminal imine group or the C-terminal amide nitrogen, respectively; (G, H) nine-membered ring isomer protonated at the N-terminal amine or ring imine nitrogen, respectively; (I–K) seven-membered ring terminated re-associated linear form protonated at the secondary amine, N-terminal amine, or ring nitrogen, respectively. The respective protonation sites are indicated by arrows. Relative ZPE-corrected energies (Gibbs free energies at 298 K) are given.

structures (G and H in Chart 3) are energetically disfavored. Similarly, the structures (I, J, and K in Chart 3) formed by re-association of the formal b_2 and imine fragments in the PBD formed by elimination of the C-terminal imine are energetically disfavored at 18–20 kcal/mol relative energy. On the other hand, the macrocyclic isomer (C in Chart 3) is energetically as favored as the linear imine terminated isomer (A in Chart 3) and the structure formed by proton transfer to the adjacent amide nitrogen (D in Chart 3) is unstable and opens up to the rearranged imine–amide isomer (E in Chart 3) which is the energetically most favored AGabaA a_3 species at approximately −13 kcal/mol relative energy.

Scheme 3 shows the dissociation pathways of the a_3 ion with the AGabaA sequence (those structures for which energies were presented in Chart 3 are labeled with the appropriate letter code). Three major reactions are considered here: (i) imine loss from structure A to form b_2 [19]; (ii) macrocycle formation, and reopening the macro-ring after proton transfer to produce the linear reordered a_3 structure E [23] and subsequent ammonia loss [26]; and (iii) formation of a proton bound dimer of b_2 and the eliminated imine, reassociation of the fragments at the N-terminus of the b_2, and elimination of ammonia, e.g. the PBD $a_3 \rightarrow a_3^*$ pathway [18].

Elimination of the C-terminal imine from a_3 requires passing a transition state at 24.8 kcal/mol relative energy (calculated using the imine protonated $AGabaA_{im}$ as reference structure). This threshold energy is significantly higher than literature $a_3 \rightarrow b_2$ values, for example Cooper et al. [18] reported 13.8 kcal/mol for the GGG $a_3 \rightarrow b_2$ reaction, whereas Glish and coworkers reported 16.7 kcal/mol barriers for both the AAAA $a_4 \rightarrow b_3$ and the AAA $a_3 \rightarrow b_2$ reactions [21]. The relatively high barrier is explained by formation of the seven-membered C-terminal ring for the AGaba b_2 ion; this structure is energetically much less favored than the isomeric GabaAox structure (see above) featuring Harrison's oxazolone ring. The relative energy of the separated products (b_2 and Ala imine) is 32.5 kcal/mol, again much higher that that calculated for the AAA case (21.4 kcal/mol [21]). These energetics means that AGabaA a_3 ion is kinetically much more stable than the AAA a_3 ion offering a reasonable explanation for the abundant a_3 peak in CID of protonated AGabaAIG (Fig. 1a).

The barrier to formation of the macrocyclic a_n isomers is 10–20 kcal/mol as reported for literature cases [10,23], so this is not likely to be the highest energy transition on the pathway of Scheme 3. Our 18.9 kcal/mol value for the macrocycle formation of the AGabaA a_3 falls well in line with these literature cases. The proton transfer to form structure D from C is however expected to be one of the rate limiting steps for this pathway due to the formal 4-atom transition structure involved. Our lowest energy proton transfer TS, from the transfer of the proton in the macrocycle to promote unfolding, is at 23.5 kcal/mol, just slightly below the threshold energy of the $a_3 \rightarrow b_2$ reaction. On the product branch of such TSs one does not locate stable D structures protonated at the amide nitrogen, rather these species spontaneously transfer to the rearranged E structure. As the energetically most favored species on the a_3 potential energy surface (PES), structure E can in principle undergo proton transfers to form the C-terminal amide nitrogen protonated form (structure F) at 14.1 kcal/mol relative energy. Such structures can eliminate ammonia by nucleophilic attack of the N-terminal adjacent carbonyl oxygen on the carbon of the protonated terminal amide bond. The relative energy of this $a_3 \rightarrow a_3^*$ TS is 22.5 kcal/mol, which is about 2 kcal/mol lower in energy than the $a_3 \rightarrow b_2$ transition state structure.

The second channel to form a_3^* is the PBD pathway that is initiated by elimination of the C-terminal imine at 24.8 kcal/mol threshold energy. We assume that subsequent rearrangements, reassociation, and PT all involve TSs at lower energies [18]. The relative energy of the resulting K structure that has the N-terminal NH_3^+-moiety is 19.6 kcal/mol and the corresponding ammonia loss TS is at 24.4 kcal/mol relative energy. This TS is lower in energy than the $a_3 \rightarrow b_2$ TS by only 0.4 kcal/mol and is about 2 kcal/mol

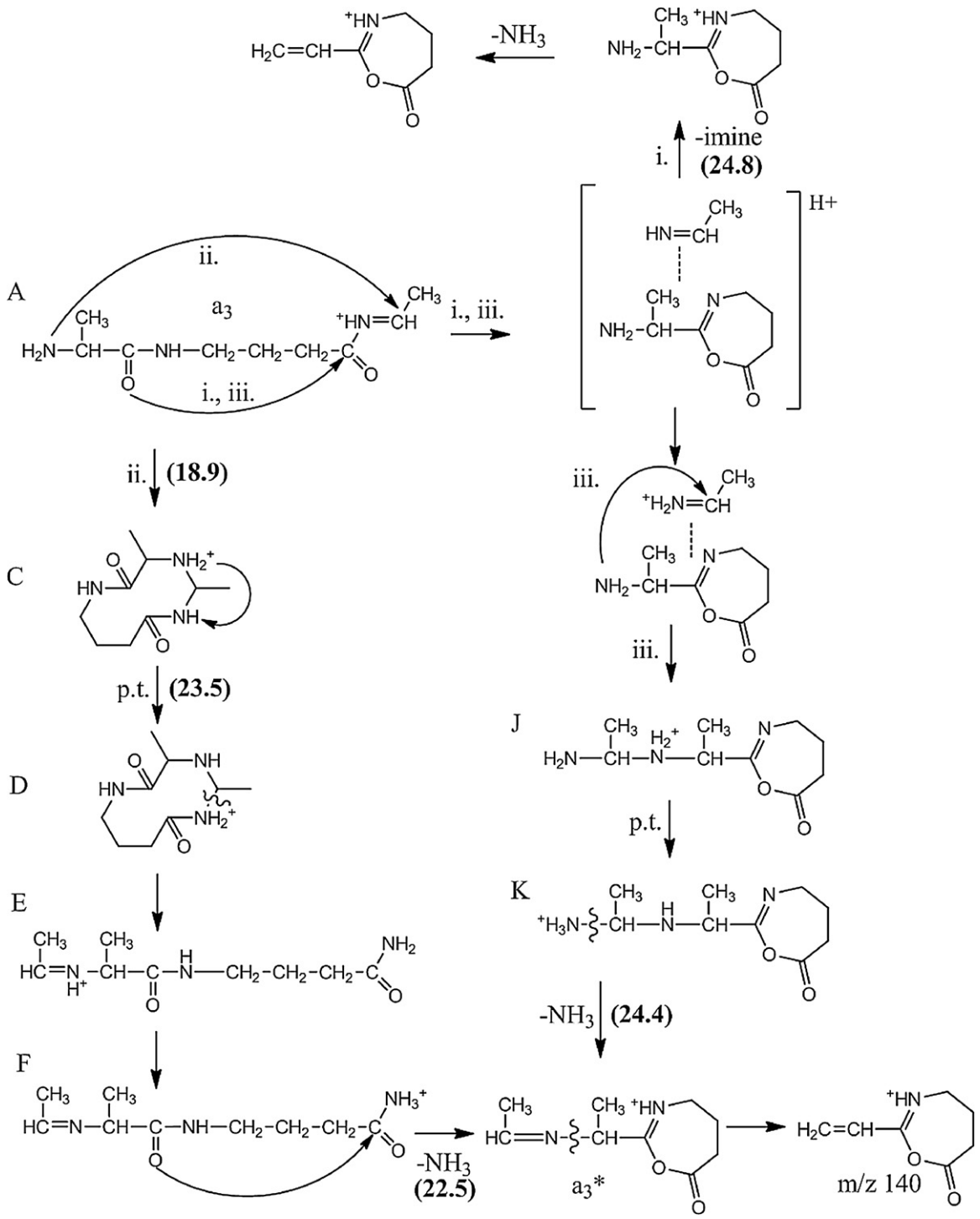

Scheme 3. Fragmentation pathways of AGabaA a_3 ion. Relevant transition state barriers reported relative to the a_3 structure A ion in kcal/mol.

higher in energy than the other ammonia loss from structure F at 22.5 kcal/mol.

The $a_3 \rightarrow b_2$ and the critical $a_3 \rightarrow a_3^*$ TSs are within 3–4 kcal/mol relative to each other for the AGabaA sequence. All these critical energies are higher than the $a_3 \rightarrow b_2$ value calculated for the AAA sequence [21]. This observation provides a reasonable explanation for the stability of the AGabaA a_3 ion; one needs to impart much more energy into this species to induce fragmentation than is necessary to dissociate the corresponding AAA a_3 ion. Furthermore, the macrocyclic AGabaA a_3 ion can undergo cyclization and possible ring-opening to form the energetically favored imine–amide isomer. Such a reaction is not possible for the AAA a_3 ion because of the energetically disfavored cyclization process. Formation of the low-energy imine–amide structure for AGabaA can be another reason for the unusually stable a_3 ion. More experimental work (such as IRMPD of the AGabaA a_3 ion) will be necessary to come to a conclusion for this phenomenon.

5. Conclusions

With an extended backbone at the second position amino acid, the intensity of the a_3 ion can be significantly increased compared

to standard alpha amino acid containing peptides. Through isotopic labeling and tandem mass spectrometry experiments, the fragments of protonated AGabaAlG were analyzed and a reaction scheme defined for the production of a_3 and its consecutive products. Modeling and DFT calculations have revealed that the a_3 ion is most likely stabilized for two distinct reasons. (i) The barrier to produce a macrocyclic structure is relative low and results in a macrocycle that is energetically as favored as the *trans* imine a_3. After proton transfer this macrocycle can unfold into an imine–amide a_3 13 kcal/mol lower in energy than the original imine isomer. (ii) The AGaba b_2 ion is energetically noticeably disfavored due to the seven-membered C-terminal ring and the transition state to form this b_2 via an imine loss is higher in energy than the similar TS calculated for the AAA sequence. Another important feature of the two methylene backbone extension was the ease with which the fragments could cyclize. In the case of the b_3, the AGabaA$_{ox}$ structure can be converted to GabaAA$_{ox}$ while this chemistry is prohibited for the AAA sequence due to the energetically disfavored macrocyclic structure. In future work, we will study the energetics and kinetics of a_3 formation for systems with varying backbone length, such as peptides with the A(βAla)A motif.

Acknowledgements

The authors would like to acknowledge funding from the NIH Grant GMR01 51387 for V.H.W. and Dennis L. Lichtenberger for his assistance in specifics on our computational work. B.P. is grateful to the Deutsche Forschungsgemeinschaft for a Heisenberg fellowship.

Appendix A. Supplementary data

Supplementary data associated with this article can be found, in the online version, at doi:10.1016/j.ijms.2012.02.028.

References

[1] B. Paizs, S. Suhai, Mass Spec. Rev. 24 (4) (2005) 508–548.
[2] L.A. Breci, D.L. Tabb, J.R. Yates, V.H. Wysocki III, Anal. Chem. 75 (9) (2003) 1963–1971.
[3] P. Roepstorff, J. Fohlmann, Proposals for a common nomenclature for sequence ions in mass spectra of peptides, Biomed. Mass Spectrom. 11 (1984) 601.
[4] K. Biemann, Contributions of mass spectrometry to peptide and protein structure, Biomed. Environ. Mass Spectrom. 16 (1988) 99–111.
[5] Wenzhou Li, Li Ji, Jonathan Goya, Guanhong Tan, Vicki H. Wysocki, SQID: an intensity-incorporated protein identification algorithm for tandem mass spectrometry, J. Proteome Res. 10 (2011) 1593–1602.
[6] A.G. Harrison, To b or not to b: the ongoing saga of peptide b ions, Mass Spectrom. Rev. 28 (2009) 640–654.
[7] N.C. Polfer, J. Oomens, S. Suhai, B. Paizs, Spectroscopic and theoretical evidence for oxazolone ring formation in collision-induced dissociation of peptides, J. Am. Chem. Soc. 127 (2005) 17154–17155.
[8] N.C. Polfer, J. Oomens, S. Suhai, B. Paizs, Infrared spectroscopy and theoretical studies on gas-phase protonated Leu-Enkephalin and its fragments: direct experimental evidence for the mobile proton, J. Am. Chem. Soc. 129 (2007) 5887–5897.
[9] S.H. Yoon, J. Chamot-Rooke, B.R. Perkins, A.E. Hilderbrand, J.C. Poutsma, V.H. Wysocki, IRMPD spectroscopy shows that AGG forms an oxazolone b_2^+ ion, J. Am. Chem. Soc. 130 (2008) 17644–17645.
[10] C. Bleiholder, S. Osburn, T.D. Williams, S. Suhai, M. Van Stipdonk, A.G. Harrison, B. Paizs, Sequence–scrambling pathways of protonated peptides, J. Am. Chem. Soc. 130 (2008) 17774–17789.
[11] U. Erlekam, B.J. Bythell, D. Scuderi, M. Van Stipdonk, B. Paizs, P. Maitre, Infrared spectroscopy of fragments of protonated peptides. Direct evidence for macrocyclic structure of b_5 ions, J. Am. Chem. Soc. 131 (2009) 11503–11508.
[12] T. Yalcin, C. Khouw, I.G. Csizmadia, M.R. Peterson, A.G. Harrison, Why are B ions stable species in peptide mass spectra? J. Am. Soc. Mass Spectrom. 6 (1995) 1165–1174.
[13] T. Yalcin, I.G. Csizmadia, M.R. Peterson, A.G. Harrison, The Structures, Fragmentation of B_n ($n \geq 3$) ions in peptide mass spectra, J. Am. Soc. Mass Spectrom. 7 (1996) 233–242.
[14] K. Ambihapathy, T. Yalcin, H.-W. Leung, A.G. Harrison, Pathways to immonium ions in the fragmentation of protonated peptides, J. Mass Spectrom. 32 (1997) 209–215.
[15] R.W. Vachet, B.M. Bishop, B.W. Erickson, G.L. Glish, Novel peptide dissociation: gas-phase intermolecular rearrangement of internal amino acid residues, J. Am. Chem. Soc. 119 (1997) 5481.
[16] R.W. Vachet, K.L. Ray, G.L. Glish, Origin of product ions in the MS/MS spectra of peptides in a quadrupole ion trap, J. Am. Soc. Mass Spectrom. 9 (1998) 341–344.
[17] B. Paizs, Z. Szlavik, G. Lendvay, K. Vekey, S. Suhai, Formation of a_2^+ ions of protonated peptides. An Ab initio study, Rapid Commun. Mass Spectrom. 14 (2000) 746.
[18] T. Cooper, E. Talaty, J. Grove, S. Suhai, B. Paizs, M. Van Stipdonk, Isotope labeling and theoretical study of the formation of a_3^* ions from protonated tetraglycine, J. Am. Soc. Mass Spectrom. 17 (2006) 1654.
[19] A.G. Harrison, A.B. Young, Fragmentation of protonated oligoalanines: amide bond cleavage and beyond, J. Am. Soc. Mass Spectrom. 15 (2004) 1810–1819.
[20] N.C. Polfer, B.C. Bohrer, M.D. Plasencia, B. Paizs, D.E. Clemmer, On the dynamics of fragment isomerization in collision-induced dissociation of peptides, J. Phys. Chem. A 112 (2008) 1286.
[21] J.M. Allen, A.H. Racine, A.M. Berman, J.S. Johnson, B.J. Bythell, B. Paizs, G.L. Glish, Why are a_3 ions rarely observed? J. Am. Soc. Mass Spectrom. 19 (2008) 1764–1770.
[22] B.J. Bythell, S. Molesworth, S. Osburn, T. Cooper, B. Paizs, M. Van Stipdonk, Structure and reactivity of a_n and a_n^* peptide fragments investigated using isotope labeling, tandem mass spectrometry, and density functional theory calculations, J. Am. Soc. Mass Spectrom. 19 (2008) 1788.
[23] B.J. Bythell, P. Maître, B. Paizs, Cyclization, Rearrangement reactions of a_n fragment ions of protonated peptides, J. Am. Chem. Soc. 132 (2010) 14766–14779.
[24] U.H. Verkerk, C.-K. Siu, J.D. Steill, H. El Aribi, J. Zhao, C.F. Rodriquez, J. Oomens, A.C. Hopkinson, K.W.M. Michael Siu, a_2 ion derived from triglycine: an N1-protonated 4-imidazolidinone, J. Phys. Chem. Lett. 1 (2010) 868–872.
[25] B.J. Bythell, P. Maître, B. Paizs, Rearrangement pathways of the a_4 ion of protonated YGGFL characterized by IR spectroscopy and modeling. J. Am. Soc. Mass Spectrom., doi:10.1007/s13361-011-0322-6, in press.
[26] B. Paizs, B.J. Bythell, A.G. Harrison, P. Maître, Structure and formation of a_n^* ions of protonated peptides, in: 59th Annual Conference on Mass Spectrometry and Allied Topics, June 5–9, 2011, Denver, CO, 2011.
[27] M.M. Savitski, M. Falth, Y.M.E. Fung, C.M. Adams, R.A. Zubarev, J. Am. Soc. Mass Spectrom. 19 (12) (2008) 1755–1763.
[28] E. Atherton, R.C. Sheppard, In Solid-Phase Peptide Synthesis: A Practical Approach, IRL Press at Oxford University Press, Oxford, UK, 1989.
[29] Asiri S. Galhena, Shai Dagan, Christopher M. Jones, Richard L. Beardsley, Vicki H. Wysocki, Surface-induced dissociation of peptides and protein complexes in a quadrupole/time-of-flight mass spectrometer, Anal. Chem. 80 (5) (2008) 1425–1436.
[30] Maestro, version 9.2, Schrödinger, LLC, New York, NY, 2011.
[31] MacroModel, version 9.9, Schrödinger, LLC, New York, NY, 2011.
[32] S.Banu Ozkan, Hagai Meirovitch, Conformational search of peptides and proteins: Monte Carlo minimization with an adaptive Bias method applied to the heptapeptide deltorphin, J. Comput. Chem. 25 (4) (2004) 565–572.
[33] M.J. Frisch, Gaussian 09, Gaussian, Inc., Wallingford, CT, 2009.
[34] A.G. Harrison, A.B. Young, C. Bleiholder, S. Suhai, B. Paizs, Scrambling of sequence information in collision-induced dissociation of peptides, J. Am. Chem. Soc. 128 (2006) 10364–10365.